

# Transcriptome profile reveals AMPA receptor dysfunction in the hippocampus of the Rsk2 knockout mice, an animal model of Coffin-Lowry syndrome

Tahir Mehmood  Anne Schneider  Jérémie Sibille  Patricia Marques Pereira   
Solange Pannetier  Mohamed Raafet Ammar  Doulaye Dembele   
Christelle Thibault-Carpentier  Nathalie Rouach  André Hanauer 

Received: 1 September 2010 / Accepted: 5 November 2010  
Springer-Verlag 2010

**Abstract** Coffin-Lowry syndrome (CLS) is a syndromic encoding proteins acting in various biological pathways, form of mental retardation caused by loss of function including cell growth and proliferation, cell death and mutations in the X-linked RPS6KA3 gene, which encodes higher brain function. The twofold up-regulated gene RSK2, a serine/threonine kinase acting in the MAPK/ERK (Gria2) was of particular interest because it encodes the pathway. The mouse invalidated for the Rps6ka3 (Rsk2 subunit GLUR2 of the AMPA glutamate receptor. AMPA KO) gene displays learning and long-term spatial memory receptors mediate most fast excitatory synaptic transmission in the central nervous system. We provide evidence gene expression profiles from Rsk2KO and normal litter-mate mice to identify changes in molecular pathways. GLUR2 at the mRNA and at the protein levels is significantly increased, whereas basal AMPA receptor-mediated transmission in the hippocampus of Rsk2KO mice is significantly decreased. This is the first time that such deregulations have been demonstrated in the mouse model of the Coffin-Lowry syndrome. Our findings suggest that a defect in AMPA neurotransmission and plasticity contribute to mental retardation in CLS patients.

T. Mehmood and A. Schneider contributed equally to this work.

Electronic supplementary material The online version of this article (doi:10.1007/s00439-010-0918-0) contains supplementary material, which is available to authorized users.

T. Mehmood · A. Schneider · P. Marques Pereira · S. Pannetier · M. R. Ammar · A. Hanauer   
Department of Translational Medicine and Neurogenetics, Institut de Génétique et de Biologie Moléculaire et Cellulaire (IGBMC), Institut National de Santé et de Recherche Médicale (INSERM) U964/Centre National de Recherche Scientifique (CNRS) UMR 7104/Université de Strasbourg, 67404 Illkirch, France  
e-mail: Andre.HANAUER@igbmc.fr

T. Mehmood  
Department of Chemistry, University of Sargodha, Sargodha 40100, Pakistan

D. Dembele · C. Thibault-Carpentier  
Microarray and Sequencing Platform, Institut de Génétique et de Biologie Moléculaire et Cellulaire (IGBMC), Institut National de Santé et de Recherche Médicale (INSERM) U964/Centre National de Recherche Scientifique (CNRS) UMR 7104/Université de Strasbourg, 67404 Illkirch, France

J. Sibille · N. Rouach  
Collège de France, 75005 Paris, France

## Introduction

Coffin-Lowry syndrome (CLS; MIM#303600) is a rare syndromic form of mental retardation that is characterized by moderate to severe psychomotor retardation, growth retardation, facial and digital dysmorphisms, as well as progressive skeletal deformations (Hanauer and Young 2002). The gene mutated in CLS patients, RPS6KA3, encodes a protein of 740 amino acids, RSK2 (alternative names: p90<sup>RSK2</sup>, MAPKAPK1B), which belongs to a family of four highly homologous proteins (RSK1-4), encoded by distinct genes. RSKs are Ser/Thr protein kinases that act at the distal end of the mitogen-activated protein kinase/extracellular signal-regulated kinases (MAPK/ERK) signaling pathway. RSKs are directly phosphorylated and activated by ERK1/2 in response to many growth factors and neurotransmitters (Firn and

Gammeltoft 1999). RSK2 phosphorylates a wide range of Microarray hybridization cytosolic substrates, such as GSK3 and nuclear substrates including ATF4, c-FOS and NUR77, CREB and histone H3 (De Cesare et al. 1998; Sassone-Corsi et al. 1999). Activation of RSK2 is, therefore, thought to influence gene expression and to be involved in cell proliferation and survival. Numerous studies implicate the MAPK/ERK signaling cascade and CREB-mediated gene transcription in synaptic plasticity and memory (Davis and Laroché 2006). In human and mouse brain, RSK2 is highly expressed in the hippocampus, that is, an essential brain structure in cognitive function and learning (Zeniou et al. 2002; Guimiot et al. 2004). RSK2-deficient mice show delayed acquisition of a spatial memory reference task and long-term spatial memory deficits (Poirier et al. 2007). Thus, together the data suggest that RSK2 plays an important role in cognitive function in human and in mice.

To gain greater insight into the molecular mechanisms leading to learning and memory impairments in Rsk2 KO mice and to mental retardation in CLS, we examined the present study global gene expression profiles in hippocampus from KO mice. The data revealed significant alteration of 100 genes acting in a great variety of biological pathway in Rsk2KO hippocampi. We further investigated the function of one of these genes, *Gria2*, which showed a twofold up-regulation in mutant mice.

*Gria2* encodes the subunit GLUR2 of the AMPA receptor (AMPA). AMPARs are ligand-activated cation channels that mediate the fast component of excitatory postsynaptic currents in neurons of the central nervous system. They are involved in several forms of long-term synaptic plasticity. Our results show that the expression of GLUR2 is increased at the mRNA and at the protein level in hippocampus, as well as at the surface of synapses in hippocampal primary cell cultures. Furthermore, basal excitatory synaptic transmission through AMPARs is impaired in the hippocampus of Rsk2 mutants.

#### Ingenuity pathways analysis

Biologically relevant networks were created using the ingenuity pathways analysis program (<http://www.ingenuity.com>), using the default parameters. Based on

#### Materials and methods

##### Animals and tissue dissection

Male Rsk2KO and WT mice with a C57Bl/6x genetic background were killed by cervical dislocation. Brains were rapidly dissected and the hippocampus was isolated using a standard dissection procedure. Tissue samples were immediately frozen in liquid nitrogen and kept at -80 °C until use. All experiments were carried out in accordance with the European Communities Council Directive of 24th November 1986 (86/609/EEC). Every effort was made to minimize the number of animals used and their suffering.

network by random chance. A score of 20 indicates that there is a  $10^{-20}$  chance that the focus genes would be in a network because of random chance.

#### Real-time QRT-PCR analysis

QRT-PCR assays were performed on hippocampal RNA samples obtained from WT and KO mice different from those used for transcriptional profiling. RNA extraction and QRT-PCR was performed as previously described (Marques Pereira et al. 2008). A probe set for detection of mouse *Gapdh* was used as an endogenous control gene.

The sequences of primers of the tested genes are listed Supplemental Table 1.

#### Western blot analysis

Protein extractions and Western blot analyses were performed as previously described (Marques Pereira et al. 2008). Quantifications were carried out with the GeneTools software of the Chemigenius apparatus (Syngene, Frederick, MD, USA). Data were normalized either to GAPDH or to  $\beta$ -TUBULIN. Student's *t* test (two-tailed) was used to determine the significance between the control

KO samples, and  $p \leq 0.05$  was considered significant. Antibodies against GLUR2 (Millipore Corporation), CACNG8 and VAMP4 (Abcam), EIF3A (Cell Signaling Technology), DIABLO (Calbiochem), GAPDH (Chemicon) and  $\beta$  TUBULIN (Millipore) were used.

#### Immunohistochemistry

Frozen brain section was left 10 min at room temperature, fixed for 10 min with 4% PFA and washed twice in PBS. Endogenous peroxidase was inhibited by a treatment with 0.3%  $H_2O_2$  solution. After washing, slides were incubated in 10% normal goat serum in  $\times 1$  PBS for 1 h. Primary antibodies were added to the sections in 10% normal goat serum and incubated overnight at 4°C. Antibody dilutions were as follows: rabbit anti-GLUR2 (1:1000, Millipore Corporation), rabbit anti-VAMP4 (1:1,000, Abcam), and rabbit anti-IGF-1 (1:100, Abcam). Slides were subsequently washed four times for 10 min in  $\times 1$  PBS and incubated with biotinylated secondary antibody for 2 h. After washing, sections were incubated for 30 min in Vectastain elite ABC reagent and treated with peroxidase substrate solution until desired stain intensity. After washing, samples were mounted with KAISER's glycerol gelatin (Merck).

#### In situ hybridization

Plasmids containing 5' UTR regions of mouse *Gria1* (encoding GLUR1) or *Gria2* (encoding GLUR2) cDNAs were

amplified by PCR using vector-specific primers and PCR reactions were purified using Montage 96 (Millipore Corporation, Bedford, USA). Amplicons were then used as template for in vitro transcription of sense and anti-sense Dig-labeled riboprobes. To this aim, 1  $\mu$ g linearized DNA was transcribed using T7, T3 or Sp6 polymerases and the DIG RNA labeling mix (Roche Diagnostics, Meylan, France) according to the manufacturer's instructions. Brain sections 25- $\mu$ m thick were processed for ISH using GenePaint robotic equipment and procedures (<http://www.genepaint.org>) as previously described (Nakamoto et al. 2007).

#### Primary hippocampal cultures

Hippocampi dissected from WT and Rsk2KO male mice at embryonic day 17 were triturated and plated into wells of 24-well plates containing poly-L-lysine-coated coverslips (Sigma), at a density of  $\sim 1,000,000$  neurons/well. Growth media consisted of NeuroBasal (GIBCO, Invitrogen) supplemented with  $\times 1$  B27 (GIBCO, Invitrogen), 0.5 mM-glutamine and  $\times 1$  penicillin/streptomycin. The cultures were maintained at 37°C in a humidified atmosphere containing 5%  $CO_2$  and cultivated for 14 DIV prior to experimentation.

#### Immunocytochemistry

To label surface GLUR1 (sGLUR1) and GLUR2 (sGLUR2)-containing AMPARs, 14 DIV live neurons were treated as previously described (Ghate et al. 2007) with minor modifications. Cells were incubated with rabbit anti-N-terminal GLUR1 (Calbiochem) or mouse anti-N-terminal GLUR2 (Millipore) and mouse anti-PSD95 (NeuroMab).

#### Microscopy and data analysis

All images acquisitions and quantifications were performed using standardized settings on a microscope (model DM4000 B, Leica) equipped with CCD camera (CoolSnap CF, color) with a  $\times 63$  objective. Obtained Tiff files were subjected to quantification with ImageJ software (<http://www.rsb.info.nih.gov/ij/>). For sGLURs quantification, the three thickest dendrites per pyramidal neuron and  $\times 3$  live neurons per sample were blindly chosen and the dendritic branches were manually traced and measured. AMPA receptors clusters were counted and the number of clusters was normalized with the dendritic length. Student's *t* tests were used for comparison between WT and Rsk2KO cultures.

#### Determination of relative *Gria2* Q/R and R/G editing, and $\beta$ ip/ $\beta$ op splice levels

Total RNA was extracted (as above) from Rsk2KO and  $\times 3$  WT hippocampi, the *Gria2* mRNA amplified by

RT-PCR (three times each from independent RNA preparations) and the product sequenced to determine relative levels of editing and splicing (Lee et al. 1998).

## Electrophysiology

Standard techniques were used to prepare transverse hippocampal slices (400  $\mu$ m thick) from 4-week-old mice. Slices were maintained at room temperature in a storage chamber that was perfused with an artificial cerebrospinal fluid (ACSF) (mM: 119 NaCl, 2.5 KCl, 1.3 MgSO<sub>4</sub>, 2.5 CaCl<sub>2</sub>, 1 NaH<sub>2</sub>PO<sub>4</sub>, 26 NaHCO<sub>3</sub> and 11 glucose and equilibrated with 95% O<sub>2</sub> and 5% CO<sub>2</sub>) for at least 1 h prior to recording. For synaptic recordings, a cut was made between the CA3 and CA1 region to prevent bursting, and the slices were bathed in a modified ACSF containing 100- $\mu$ m picrotoxin to block GABA<sub>A</sub> receptor-mediated inhibitory postsynaptic currents. Field excitatory postsynaptic potentials (fEPSPs) were recorded with glass pipettes (205 M $\Omega$ ) filled with ACSF, by stimulating Schaffer collaterals in stratum radiatum (0.1 Hz) with a monopolar stimulating electrode. Responses were collected with Axopatch-1D amplifier (Axon Instruments), filtered at 2 kHz, digitized at 10 kHz, and analyzed online using Clampfit software (Molecular Devices).

Validation of microarray data by QRT-PCR

Twenty-four of these differentially expressed genes were selected for validation, by QRT-PCR, based on the known putative neuronal functional roles (Table 1). These genes represent different categories: genes implicated in ataxocytosis (*Atx1* and *Vamp4*), in mental retardation (*Cul4b*, *Lamp2*, *Vldlr*, *Igf1*), in apoptosis (*Itk3*, *Rasl10a*, *Diablo*), in cell differentiation and cytoskeleton organization (*Phkg1*, *Pdlim5*, *Timsb10*, *Enc1*, *Nptxr*, *Ptpn2*, *Carhsp1*, *Phip*, *Plek*, *Arhgap12*, *C3b1*), in translation regulation (*Eif3A*) and finally genes encoding ion channel sub-units (*Cacnb4*, *Cacng8*, *Gria2*). The results of the microarray findings were validated in all the genes tested by real-time PCR, although the fold change was not always accurately replicated. We also confirmed by QRT-PCR unaltered expression of some genes (including *cFos*, *CREB*) that had similar levels of expression in KO and WT animals on six microarrays (results not shown).

## Results

### Expression profiling of wild-type and *Rsk2*KO mice

To identify molecular changes potentially responsible for the phenotype associated with *RSPS6KA3* gene mutation in the hippocampus, we performed a detailed comparison of the transcriptional profiles of hippocampi isolated from six KO and six WT 5-month-old male mice. To reduce variability, equivalent amounts of RNA from two mice with the same genotype were pooled and processed for hybridization to the genome wide oligonucleotide microarray (thus, three arrays per genotype). Out of the 22,690 probesets represented on the microarray, 16,865 probesets that were restricted to 14,348 probesets by filter a and to 635 probesets by filter b and to 635 probesets by filter c. Filter d, selected a total number of 109 probesets. Eight of these 109 differentially expressed genes were verified by two or, in one case, three distinct probe sets. These multiple probe sets eight genes displayed consistent direction and similar extent of changes in abundances of corresponding mRNAs. The final list of 100 significant non-redundant genes is shown in Table 1. Genes are tabulated according to functional category and degree of over-expression/repression.

Identification of biologically relevant networks

To gain insight into interactions among the differentially expressed genes, we constructed biologically relevant networks using the ingenuity pathway analysis software. From the 100 differentially expressed genes, 78 genes were mapped and assembled into five biological networks with a *P*-value of  $\geq 20$ . The network with the most significant score (of 45) contains 23 of the differentially expressed genes. This network contains genes involved in cell cycle, cellular development, growth and proliferation and centers on the NF- $\kappa$ B complex. This network contains also *Rb1* and *Sod2*, both important actors in cellular growth and apoptosis, and *Rsk2* which controls proliferation, cellular differentiation, but also various other functions. Fourteen genes with altered

Table 1 List of genes differentially expressed in the hippocampus of Rsk2-KO mice

Functional category	Probe set	Genbank	Gene symbol	Gene name	Microarray		qRT-PCR		FC	p
					FC KO/WT	p	WT mean Ct ± SD	KO mean Ct ± SD		
Genes showing decreased expression										
Kinases	1422315_x_at	NM_011079	Phkg1	Phosphorylase kinase gamma 1	0.54	0.0162	± 0.03	0.68 ± 0.11	0.68	0.003
	1418052_at	NM_023556	Mvk	Mevalonate kinase	0.55	0.0190				
Enzymes	1427282_a_at	NM_008044	Fxn	Frataxin	0.61	0.0074				
	1448330_at	NM_010358	Gstm5	Glutathione S-transferase M5	0.61	0.023				
	1427975_at	NM_145216	Ras10a	Ras-like, family 10, member A	0.62	0.015	± 0.05	0.70 ± 0.059	0.70	0.004
	1433918_at	NM_034941	Atg4d		0.59	0.0057				
Peptidase	1418345_at	NM_023517	Trnslf13	Tumor necrosis factor (ligand) superfamily, member 13	0.60	0.0057				
	1418636_at	NM_001083318	Ev3	Ets variant gene 3	0.55	0.026				
Transcription regulator	1423927_at	NM_028662	Slc35b2	Solute carrier family 35, member B2	0.59	0.011				
	1450073_at	NM_008444	Kif3b	Kinesin family, member 3B	0.64	0.00093				
Transporters	1450147_at	NM_030689	Nptxr	Neuronal pentraxin receptor	0.62	0.013	± 0.008	0.87 ± 0.35	0.87	0.035
	1452406_x_at	NM_133362	Erd1	Erythroid differentiation regulator 1	0.35	0.029				
Other functions	1417909_at	NM_080844	Serpinc1	Serpin peptidase inhibitor, clade C, member 1	0.41	0.023				
	1415976_a_at	NM_025821	Carhsp1	Calcium regulated head stable protein 1, 24 kDa	0.50	0.00036	± 0.007	0.63 ± 0.07	0.63	0.034
	1452652_a_at	NM_001002267	Tmem158	Transmembrane protein 158	0.55	0.015				
	1448577_x_at	NM_009304	Syng2	Synaptogyrin 2	0.56	0.021				
	1450098_a_at	NM_011707	Vtn	Vitronectin	0.57	0.0022				
	1453111_a_at	NM_026542	Slc25a39	Solute carrier family 25, member 39	0.61	0.011				
	1418396_at	NM_134116	Gpsm3	G-protein signaling modulator 3	0.63	0.016				
	1423940_at	NM_026553	Yif1A	Yip1 interacting factor homolog AS, cerevisiae	0.63	0.016				
	1418123_at	NM_011676	Unc119	Unc-119 homolog C, elegans	0.64	0.0016				
	1450468_at	NM_010865	Myoc	Myocilin	0.64	0.0078				
Genes showing increased expression										
Kinases	1418513_at	NM_019635	Stk3	SH2 domain containing 3C	0.64	0.001				
	1438562_a_at	NM_021426	Nkain4	Na+/K+ transporting ATPase interacting 4	0.65	0.022				
Phosphatase	1437401_at	NM_010512	Igf1	Cdc42 GTPase-activating protein	0.65	0.009				
	1417069_a_at	NM_022023	Gmfb	Serine/threonine kinase 3	1.76	0.023	± 0.05	1.45 ± 0.08	1.45	0.042
Growth factors	1437401_at	NM_010512	Igf1	Protein tyrosine phosphatase, non-receptor type 2	1.95	0.016	± 0.091	1.85 ± 0.28	1.83	0.045
	1417069_a_at	NM_022023	Gmfb	Insulin-like growth factor 1	1.65	0.0093	± 0.09	2.24 ± 0.32	2.24	0.042
				Maturation factor, beta	1.54	0.0055				

Table 1 continued

Functional category	Probe set	Genbank	Gene symbol	Gene name	Microarray		qRT-PCR		FC	P	KO mean	FC	P	
					F C	P	WT mean	Ct ± SD						KO mean
Enzymes	1448734_at	NM_001042611	Cp	Ceruloplasmin	2.29	0.029								
	1417262_at	NM_011198	Ptgs2	Prostaglandin-endoperoxidase synthase 2	2.28	0.0047								
	1452484_at	NM_053070	Ca7	Carbonic anhydrase VII	2.23	0.028								
	1417194_at	NM_013671	Sod2	Superoxide dismutase 2	1.98	0.0089								
	1452158_at	NM_029735	Eprs	Glutamyl-prolyl-tRNA synthetase	1.95	0.015								
	1453928_a_at	NM_009278	Ssb	Sjogren syndrome antigen B	1.86	0.020								
	1451436_at	NM_001081203	Sbno1	sno, strawberry notch homolog D(sophila)	1.78	0.022								
	1454696_at	NM_008142	Gnb1	Guanine nucleotide binding protein, beta polypeptide 1	1.70	0.0016 ± 0.0033	1.36 ± 0.061	1.36	0.0005					
	1419064_a_at	NM_011674	Ugt8	UDP-glycosyltransferase 8	1.69	0.0059								
	1416497_at	NM_009787	Pdia4	Protein disulfide isomerase family A, member 4	1.68	0.0061								
	1423033_at	NM_008408	Stt3a	Subunit of the oligosaccharyltransferase complex, homolog A	1.66	0.028								
	1435164_s_at	NM_011666	Ube1c	Ubiquitin-activating enzyme E1C	1.65	0.0062								
	145388_at	NM_183028	Pcmd1	protein-L-isoaspartate-methyltransferase domain containing 1	1.60	0.026								
	1416343_a_at	NM_010685	Lamp2	Lysosomal-associated membrane protein 2	1.58	0.023 ± 0.005	1.65 ± 0.19	1.65	0.038					
	1418908_at	NM_013626	Pam	Peptidylglycine alpha-amidating monoxygenase	1.56	0.021								
	1451828_a_at	NM_207625	Acs14	Acyl-CoA synthetase long chain family member 4	1.54	0.0035								
	1417697_at	NM_009230	Soat1	Sterol O-acyltransferase	1.51	0.015								
	Peptidase	1420964_at	NM_007930	Enc1	Ectodermal-neural cortex	2.07	0.015	1.77 ± 0.08	1.77	0.002				
		1449718_s_at	NM_026273	C3orf38	Chromosome 3 open reading frame 38 homolog (human)	1.54	0.019							
Transcription regulators	1427406_at	NM_028446	Trp11	Thyroid hormone receptor interactor 11	2.27	0.0045								
	1423501_at	NM_008558	Max	MYC-associated factor X	1.91	0.023								
	1417187_at	NM_016786	Hip2	Huntington interacting protein 2	1.76	0.0071								
	1424704_at	NM_001145920	Runx2	Runt-related transcription factor 2	1.67	0.0068								
	1418265_s_at	NM_008391	Irf2	Interferon regulatory factor	1.60	0.023								
	1417850_at	NM_009029	Rb1	Retinoblastoma 1	1.58	0.0053								
	1416661_at	NM_010123	Eif3a	Eukaryotic translation initiation factor 3, subunit A	1.74	0.0087 ± 0.005	1.84 ± 0.11	1.84	0.005					
	1422631_at	NM_013484	Ahr	Aryl hydrocarbon receptor	1.61	0.028								
	1416958_at	NM_011584	NhrD2	Nuclear receptor subfamily 1, group D, member 2	1.54	0.0064								
	1422966_a_at	NM_011638	Tfrc	Transferrin receptor	2.10	0.0010								
Transporters	1416653_at	NM_011504	Sixbp3	Syntaxin-binding protein 3	1.92	0.013	2.19 ± 0.6	2.19	0.038					
	1442169_at	NM_013703	Vldlr	Very low density lipoprotein receptor	1.79	0.0068 ± 0.005	1.44 ± 0.055	1.44	0.0007					
	1424924_at	NM_153055	Sec63	SEC63 homolog, cerevisiae	1.74	0.015								
	1419975_at	NM_011327	Scp2	Sterol carrier protein 2	1.66	0.023								
	1416374_at	NM_018829	Ap3m1	Adaptor-related protein complex 3 mu 1 subunit	1.59	0.0032								
	1434513_at	NM_001128096	Atp13a3	ATPase type 13A3	1.52	0.0054								
	1453098_at	NM_013540	Gria2	Glutamate receptor, ionotropic, AMPA2	2.01	0.024	± 0.032	1.87 ± 0.09	1.87	0.0003				
	1452089_at	NM_001037099	Caenb4	Calcium channel, voltage-dependent, beta 4 subunit	1.85	0.003 ± 0.022	1.34 ± 0.02	1.34	0.022					
	1451864_at	NM_133190	Caenb8	Calcium channel, voltage-dependent, gamma subunit 8	1.79	0.012 ± 0.08	1.84 ± 0.26	1.84	0.005					

Table 1 continued

Functional category	Probe set	Genbank	Gene symbol	Gene name	Microarray		qRT-PCR		FC	p	FC	p
					F C	p	WT mean Ct ± SD	KO mean Ct ± SD				
Other functions	1455946_x_at	NM_001039392	Tnusb10	Thymosin, beta 10	3.51	0.0052	± 0.04	2.56 ± 0.05	2.56	0.028		
	1424325_at	NM_001081222	Escot1	Establishment of cohesion 1 homolog	2.91	0.024						
	1425768_at	NM_023232	Diablo	Diablo homolog (Drosophila)	2.05	0.023	1 ± 0.032	2.16 ± 0.05	2.16	0.0002		
	1455475_at	NM_026622	C4orf29	Chromosome 4 open reading frame 29 homolog (human)	2.00	0.023						
	1423198_a_at	NM_134034	Smek2	SMEK homolog 2, suppressor of mek1 (Dictyostelium)	1.93	0.014						
	1424074_at	NM_027453	Btf3l4	Basic transcription factor 3-like 4	1.88	0.018						
	1420485_at	NM_023554	Nol7	Nucleolar protein 7	1.78	0.016						
	1438418_at	NM_144535	Mudeng	MU-2/AP1M2 domain containing, death-inducing	1.77	0.014						
	1421945_a_at	NM_001042556	Bxdc1	Brix domain containing 1	1.77	0.0077						
	1450418_a_at	NM_026553	Yif1a	Yip1-interacting factor homolog	1.74	0.029						
	1449884_at	NM_026626	Efcab2	EF-hand calcium binding domain 2	1.71	0.020						
	1418008_at	NM_026110	C21orf66	Chromosome 21 open reading frame 66 homolog (human)	1.68	0.023						
	1438535_at	NM_001081216	Phip	Pleckstrin homology domain interacting protein	1.65	0.01 ± 0.19		2.08 ± 0.09	2.08	0.03		
	1451525_at	NM_001039692	Athgap12	Rho GTPase-activating protein 12	1.64	0.020 ± 0.09		1.54 ± 0.09	1.54	0.033		
	1426271_at	NM_153808	Smc5	Structural maintenance of chromosome 5	1.63	0.015						
	1417170_at	NM_033322	Lztf3	Leucine zipper transcription factor-like 1	1.62	0.029						
	1452247_at	NM_001113188	Fxr1	Fragile X mental retardation, autosomal homolog 1	1.62	0.0047						
	1451325_at	NM_027226	Fyft1d	Forty-two three domain containing 1	1.61	0.0050						
	1425913_a_at	NM_144882	Dnaptip6	Viral DNA polymerase-trans-activated protein 6	1.60	0.012						
	1421940_at	NM_009282	Stag1	Stromal antigen 1	1.59	0.011						
	1448748_at	NM_019549	Plek	Pleckstrin	1.58	0.021 ± 0.05		1.12 ± 0.09	1.12	0.004		
	1451830_a_at	NM_009260	Spnb2	Spectrin, beta, non-erythrocytic 1	1.58	0.019						
	1437463_x_at	NM_011577	Tgfb1	Transforming growth factor, beta-induced	1.57	0.016						
	1423841_at	NM_026396	Bxdc2	Brix domain containing 2	1.57	0.026						
1427104_at	NM_175480	Znf23	Zinc finger protein 612	1.56	0.015							
1426806_at	NM_028696	Obfc2a	Oligonucleotide/oligosaccharide-binding fold containing 2A	1.55	0.023							
1422896_at	NM_016796	Vamp4	Vesicle-associated membrane, protein 4	1.55	0.01 ± 0.07		1.48 ± 0.16	1.48	0.034			
1437790_at	NM_001081191	Emi5	Vesicle-associated membrane associated protein like 5	1.54	0.020							
1417453_at	NM_001110142	Cul4b	Echinoderm microtubule associated protein like 5	1.53	0.028 ± 0.03		1.12 ± 0.09	1.12	0.018			
1418066_at	NM_007688	C62	Cullin 4B	1.53	0.019							
1450407_a_at	NM_009672	Anp32a	Acidic nuclear phosphoprotein 32 family, member A	1.53	0.013							
1450786_at	NM_019808	Pdlim5	PDZ and LIM domain 5	1.53	0.0057 ± 0.11		1.44 ± 0.059	1.44	0.047			
1425597_a_at	NM_021881	Qk	Quaking homolog, KH domain RNA binding	1.52	0.029							

Real-time quantitative RT-PCR was performed for 24 genes in hippocampal CA1 of KO (n = 6) and WT (n = 6) mice, using the primer pairs shown in Table S1. Relative expression levels are shown with the average expression value of the WT group set to 1.

Ct cycle threshold values ± SD standard deviation; FC fold change, p p value

expression in Rsk2KO mice are associated with this second network, among which Nptxr, Cacng8, Pdlim5 and Soat1. The third network centered on MYC is mainly the twofold increased level of expression of Gria2, implicated in lipid metabolism and cell death. Thirteen encoding the subunit GLUR2 of the AMPAR. Since AMPARs mediate fast synaptic transmission at excitatory synapses in the brain and are thought to play key roles in learning and memory (Seidenman et al. 2003) we wanted to further confirm up-regulation of the protein synthesis (5th network). The fourth network is centered on Ptgs2 and includes 12 focus genes, among which Igf1, Vamp4, Mvk, Stxbp3 and Gnb1. The fifth network is centered on retinoic acid and contains 13 focus genes, among which Cacnb4 and Carhsp1. We did not find any change in the level of expression of related biological functions and diseases. Top biological functions include organismal injury and abnormalities (9 genes, including Fxn, Sod2, Igf1, Ahr and Ptgs2), cell cycle (12 genes including Rb1, Igf1 and Runx2), nervous system development and function (10 genes including Ptgs2, Sod2, Gria2, Vldlr, Vtn and Rb1), organismal development and free radical scavenging (9 and 4 genes, respectively). Interestingly, Ptgs2, Sod2 and Vldlr have been implicated in behavior, with the first four genes specifically in spatial memory formation. These five genes are all up-regulated in the hippocampus of Rsk2KO mice. The p values in the range of  $2.52 \times 10^{-5}$  to  $1.10 \times 10^{-2}$  indicate statistical significance.

#### Confirmation of altered expression at the protein level

We confirmed increased expression at the protein level of GLUR2 (Gria2 gene), CACNG8, VAMP4, EIF3A and DIABLO using quantitative western blot analysis (Fig. 2).

These findings are in line with the changes detected by microarray-based analysis. We also confirmed differential expression of GLUR2, VAMP4 and IGF1 using immunohistochemical analysis. As shown in Fig. 3, we found increased expression of GLUR2 in the CA1 and CA3 regions and in the dentate gyrus of Rsk2KO hippocampus. Although the lack of specific antibodies precluded similar experimental validations for many other genes listed in Table 1, these observations suggested that the transcriptional changes observed in mutant mice may be generally reflected by matching changes in the levels of expression of their corresponding protein products.

Confirmation by in situ hybridization of Gria2 up-regulation

The expression of a number of genes involved in neurotransmission, including vesicle and receptor trafficking site editing and  $\beta$ ip/ $\beta$ op splice levels of the

expression in Rsk2KO mice are associated with this second network, among which Nptxr, Cacng8, Pdlim5 and Soat1. The third network centered on MYC is mainly the twofold increased level of expression of Gria2, implicated in lipid metabolism and cell death. Thirteen encoding the subunit GLUR2 of the AMPAR. Since AMPARs mediate fast synaptic transmission at excitatory synapses in the brain and are thought to play key roles in learning and memory (Seidenman et al. 2003) we wanted to further confirm up-regulation of the protein synthesis (5th network). The fourth network is centered on Ptgs2 and includes 12 focus genes, among which Igf1, Vamp4, Mvk, Stxbp3 and Gnb1. The fifth network is centered on retinoic acid and contains 13 focus genes, among which Cacnb4 and Carhsp1. We did not find any change in the level of expression of related biological functions and diseases. Top biological functions include organismal injury and abnormalities (9 genes, including Fxn, Sod2, Igf1, Ahr and Ptgs2), cell cycle (12 genes including Rb1, Igf1 and Runx2), nervous system development and function (10 genes including Ptgs2, Sod2, Gria2, Vldlr, Vtn and Rb1), organismal development and free radical scavenging (9 and 4 genes, respectively). Interestingly, Ptgs2, Sod2 and Vldlr have been implicated in behavior, with the first four genes specifically in spatial memory formation. These five genes are all up-regulated in the hippocampus of Rsk2KO mice. The p values in the range of  $2.52 \times 10^{-5}$  to  $1.10 \times 10^{-2}$  indicate statistical significance.

We next wondered whether expression of GLUR2 at surface of synapses was also up-regulated since AMPARs in hippocampal neurons are mainly expressed as heteromers (Gria2, 3 and 4 subunits undergo RNA editing (arginine to glycine) at codon 764 (in GLUR2) (Lomeli et al. 1994). The pre-messenger RNA transcripts of all the four GLUR subunits can finally be alternatively spliced to produce either the  $\beta$ ip or  $\beta$ op isoforms. Because the level of expression of GLUR2 was increased in Rsk2KO mice, we wondered whether Gria2 RNA editing and splicing were altered.

To determine whether there are changes in the Q/R, R/G editing and  $\beta$ ip/ $\beta$ op splice levels of the

GLUR2 surface staining was punctate (Fig. 4a, b), and the number of GLUR2 puncta that were synaptic did significantly differ among WT and Rsk2KO cultures (WT  $8.1 \pm 1.4$ , n = 12 embryos, KO  $14.9 \pm 2.2$ , n = 12, p = 0.015). This provided evidence that increase in total GLUR2 was correlated with increased surface-expressed GLUR2. No significant difference of surface GLUR1 was detected (WT  $12.4 \pm 7.4$ , n = 4, KO  $10.7 \pm 5$ , n = 6, p = 0.8) (Supplemental Fig. 1).

Determination of relative Gria2 R/G editing and  $\beta$ ip/ $\beta$ op splice levels

The great majority of native AMPA receptors are impermeable to calcium ions, due to the presence of the GLUR2 subunit. This subunit confers calcium impermeability on the channel due to RNA editing of a glutamine (Q) to an arginine (R) at codon 607. In addition to the Q/R site in GLUR2, the 3 and 4 subunits undergo RNA editing (arginine to glycine) at codon 764 (in GLUR2) (Lomeli et al. 1994). The pre-messenger RNA transcripts of all the four GLUR subunits can finally be alternatively spliced to produce either the  $\beta$ ip or  $\beta$ op isoforms. Because the level of expression of GLUR2 was increased in Rsk2KO mice, we wondered whether Gria2 RNA editing and splicing were altered.

To determine whether there are changes in the Q/R, R/G editing and  $\beta$ ip/ $\beta$ op splice levels of the

GLUR2 surface staining was punctate (Fig. 4a, b), and the number of GLUR2 puncta that were synaptic did significantly differ among WT and Rsk2KO cultures (WT  $8.1 \pm 1.4$ , n = 12 embryos, KO  $14.9 \pm 2.2$ , n = 12, p = 0.015). This provided evidence that increase in total GLUR2 was correlated with increased surface-expressed GLUR2. No significant difference of surface GLUR1 was detected (WT  $12.4 \pm 7.4$ , n = 4, KO  $10.7 \pm 5$ , n = 6, p = 0.8) (Supplemental Fig. 1).

Determination of relative Gria2 R/G editing and  $\beta$ ip/ $\beta$ op splice levels

The great majority of native AMPA receptors are impermeable to calcium ions, due to the presence of the GLUR2 subunit. This subunit confers calcium impermeability on the channel due to RNA editing of a glutamine (Q) to an arginine (R) at codon 607. In addition to the Q/R site in GLUR2, the 3 and 4 subunits undergo RNA editing (arginine to glycine) at codon 764 (in GLUR2) (Lomeli et al. 1994). The pre-messenger RNA transcripts of all the four GLUR subunits can finally be alternatively spliced to produce either the  $\beta$ ip or  $\beta$ op isoforms. Because the level of expression of GLUR2 was increased in Rsk2KO mice, we wondered whether Gria2 RNA editing and splicing were altered.

To determine whether there are changes in the Q/R, R/G editing and  $\beta$ ip/ $\beta$ op splice levels of the

GLUR2 surface staining was punctate (Fig. 4a, b), and the number of GLUR2 puncta that were synaptic did significantly differ among WT and Rsk2KO cultures (WT  $8.1 \pm 1.4$ , n = 12 embryos, KO  $14.9 \pm 2.2$ , n = 12, p = 0.015). This provided evidence that increase in total GLUR2 was correlated with increased surface-expressed GLUR2. No significant difference of surface GLUR1 was detected (WT  $12.4 \pm 7.4$ , n = 4, KO  $10.7 \pm 5$ , n = 6, p = 0.8) (Supplemental Fig. 1).

Determination of relative Gria2 R/G editing and  $\beta$ ip/ $\beta$ op splice levels

The great majority of native AMPA receptors are impermeable to calcium ions, due to the presence of the GLUR2 subunit. This subunit confers calcium impermeability on the channel due to RNA editing of a glutamine (Q) to an arginine (R) at codon 607. In addition to the Q/R site in GLUR2, the 3 and 4 subunits undergo RNA editing (arginine to glycine) at codon 764 (in GLUR2) (Lomeli et al. 1994). The pre-messenger RNA transcripts of all the four GLUR subunits can finally be alternatively spliced to produce either the  $\beta$ ip or  $\beta$ op isoforms. Because the level of expression of GLUR2 was increased in Rsk2KO mice, we wondered whether Gria2 RNA editing and splicing were altered.

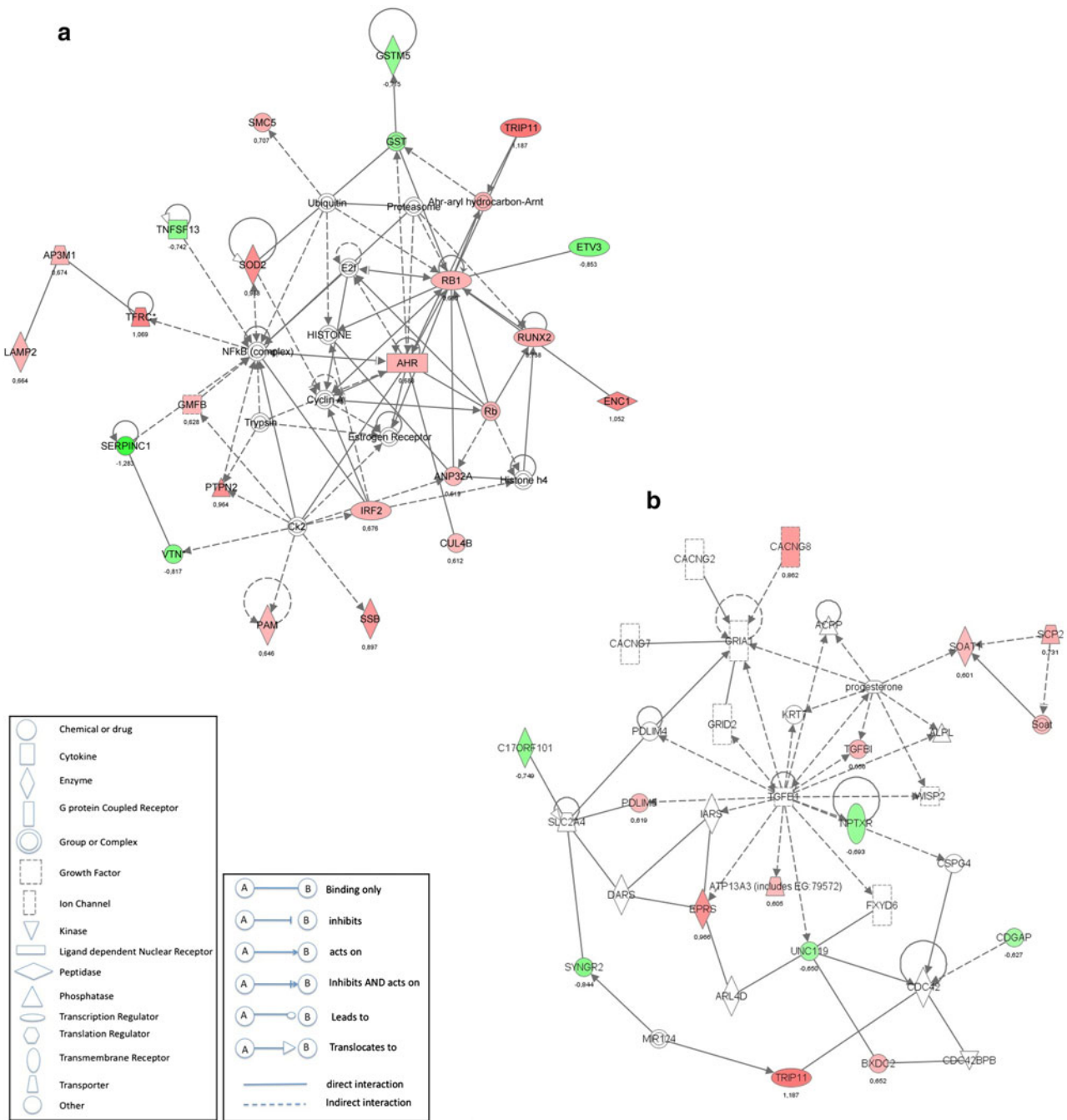
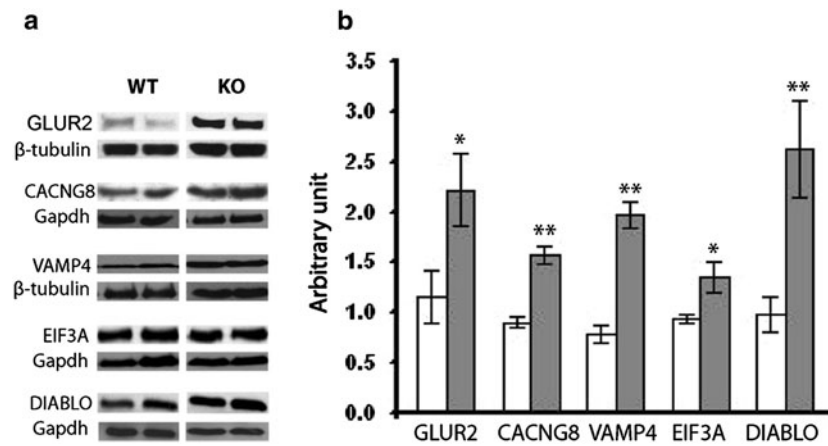
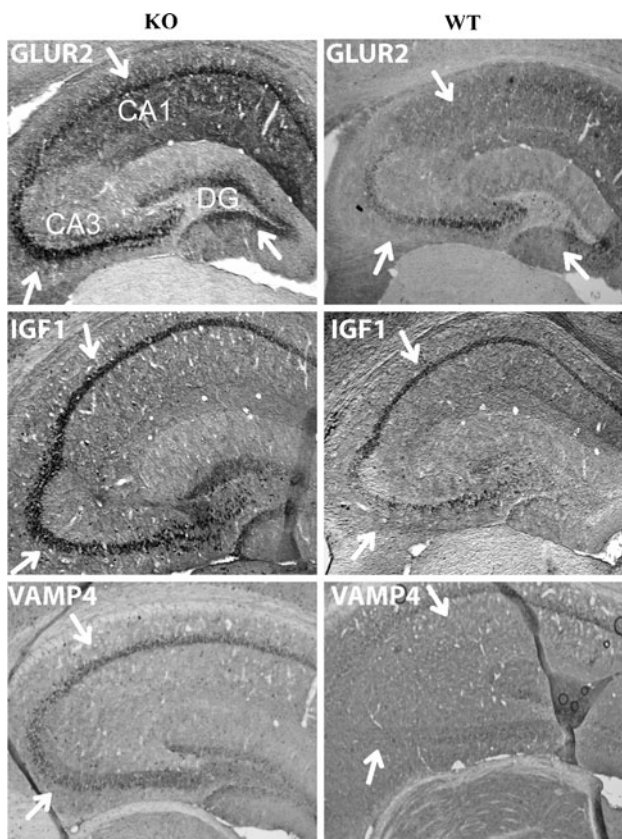


Fig. 1 Top integrated networks dysregulated in the hippocampus of Rsk2KO mice. a This network is centered on RB1. Twenty-six differentially expressed focus genes were brought into this network with a score of 0.15. b This network is centered on TGFBI. Fifteen differentially expressed focus genes were brought into this network with a score of 0.15. Nodes and edges are described below the networks

messenger in 5-month-old Rsk2KO hippocampi, the *Gria2* mRNA from pveRsk2KO and pve WT hippocampi was amplified by RT-PCR and the products sequenced to determine the relative levels of editing and splicing (Lee et al. 1998). No unedited form of the *Gria2* transcript at the Q/R site (codon 607) was detectable (not shown) neither in Rsk2KO nor in WT mice, suggesting that the amount is very low. These data are in accordance with the previously reported results indicating that editing of Q/R site is 99% complete (Carlson et al. 2000). At the R/G editing site (codon 764) edited (codon GGA) and unedited (codon GGA) forms were detectable in both WT and mutant mice.



**Fig. 2** Quantitative Western blot analyses. Levels of protein either to GAPDH or to  $\beta$ -TUBULIN are represented as the expressed by the five up-regulated genes assayed are significantly  $p < 0.05$  and \*\* $p < 0.01$  in Rsk2KO mice. a Proteins detected in two Rsk2KO and two WT mice are shown. b Data normalized to GAPDH or  $\beta$ -TUBULIN. Error bars represent  $\pm$  SEM for six mice of each genotype for GLUR2 and CACNG8 and four mice for EIF3A, VAMP4 and DIABLO. WT white bar, KO gray bar. \* $p < 0.05$  and \*\* $p < 0.01$



**Fig. 3** Immunohistochemical analysis. Proteins expressed by three up-regulated genes show significantly higher expression in Rsk2KO mice hippocampus. Three mice for each genotype were analyzed. Each picture represents one of the triplicate. Arrows point to hippocampus sub-regions showing increased expression in KO versus WT mice. CA1, CA3 and DG (dentate gyrus): hippocampus sub-regions

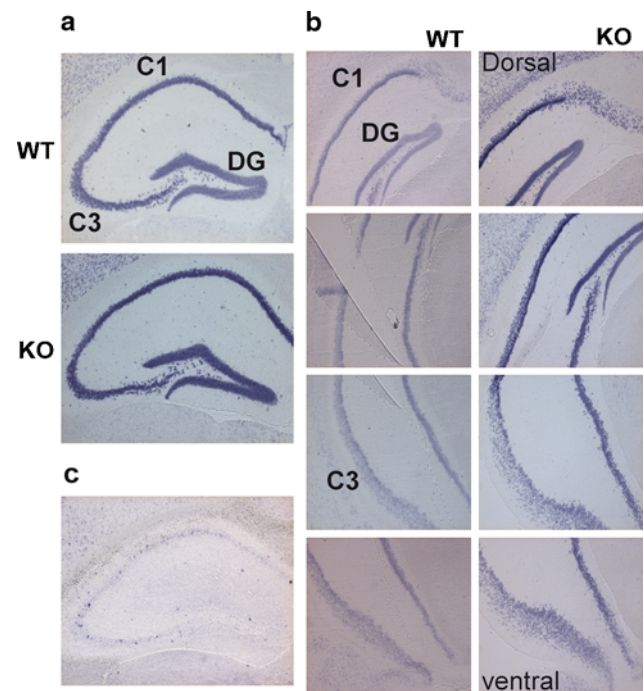


**Fig. 4** In situ hybridization. Dig-labeled Gria2 sense and anti-sense RNAs were hybridized to 25  $\mu$ m coronal sections of three Rsk2KO and three WT adult mouse brains. One picture from each genotype is shown. a Significantly increased expression in all areas of the anterior hippocampus of Rsk2KO mice. b In the posterior hippocampus the level of Gria2-mRNA was mainly increased in the dentate gyrus, in CA1 and in the ventral CA3 region. No staining was observed with sense RNA

The peak intensity of the G nucleotide signal at the edited position was measured and reported as a percentage of the total signal (A and G). Representative chromatograms from WT mice are in accordance with the previous reports (one KO and one WT littermate are shown in Supplementary Fig. 2). In WT hippocampi, the Gria2 mRNA was approximately 61  $\pm$  4% edited, whereas there was less editing in the Rsk2KO hippocampi (43  $\pm$  3%,  $p = 0.005$ ). Our data for Rsk2KO mice are in accordance with the previous reports

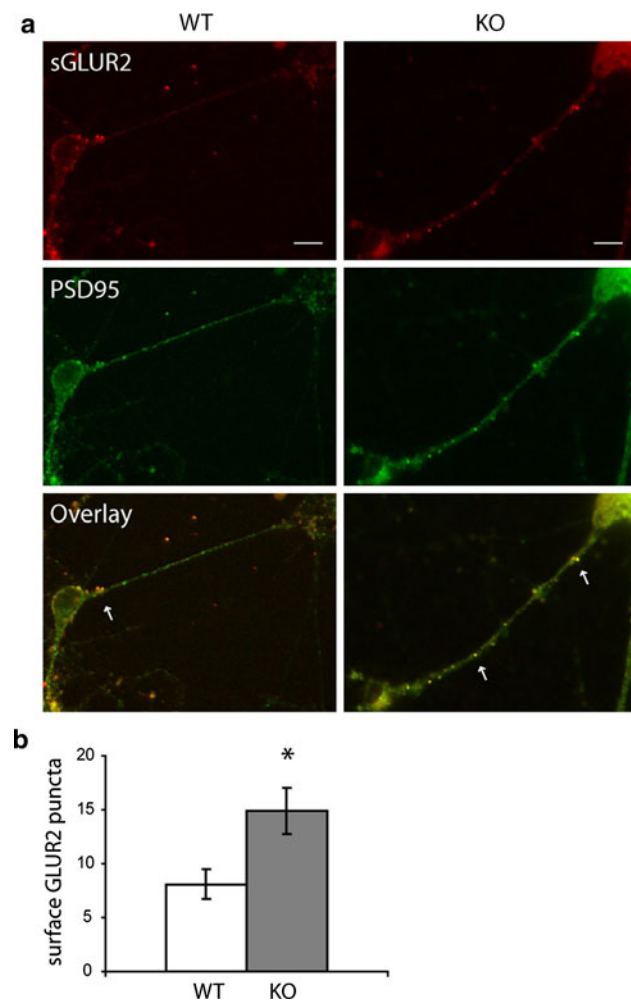


**Fig. 5** Surface expression of AMPARs. WT and Rsk2KO hippocampal neurons were labeled with N-terminal GLUR2 antibody under non-permeabilized condition to stain surface GLUR2 (sGLUR2), followed by PSD95 staining (a post-synaptic marker). Arrowpoint to post-synaptic surface-expressed GLUR2. Scale bar 10  $\mu$ m. **b** Quantification of sGLUR2 puncta. Data represent mean  $\pm$  SEM of detected sGLUR2 clusters per unit dendrite length, from 12 (WT) and 12 (KO) embryos.  $p < 0.05$

demonstrating an editing status at the R/G site of approximately 64% (Lai et al. 1997). Thus, in Rsk2KO mice the extent of R/G editing was significantly decreased (relative decrease: 18%,  $p = 0.003$ ) in the hippocampal tissue.

To determine the ratio of transcripts in the  $\beta$ ip/ $\beta$ op form, the peak intensity of the alternative splice form, the nucleotide difference (C vs. A) between the two variants was measured (Lee et al. 1998). In the WT hippocampi, there were approximately 55% of Glur2 transcript in the  $\beta$ ip form, whereas the percentage was significantly lower ( $43 \pm 3\%$ ,  $p = 0.002$ ) in the Rsk2KO hippocampi (Supplemental Fig. 2c, d). No significant difference for the Gria1 mRNA (encoding GLUR1) for the R/G editing site or  $\beta$ ip/ $\beta$ op splice levels was found between WT and mutant mice (Supplemental Fig. 2a, b).

## Reduced AMPA synaptic transmission

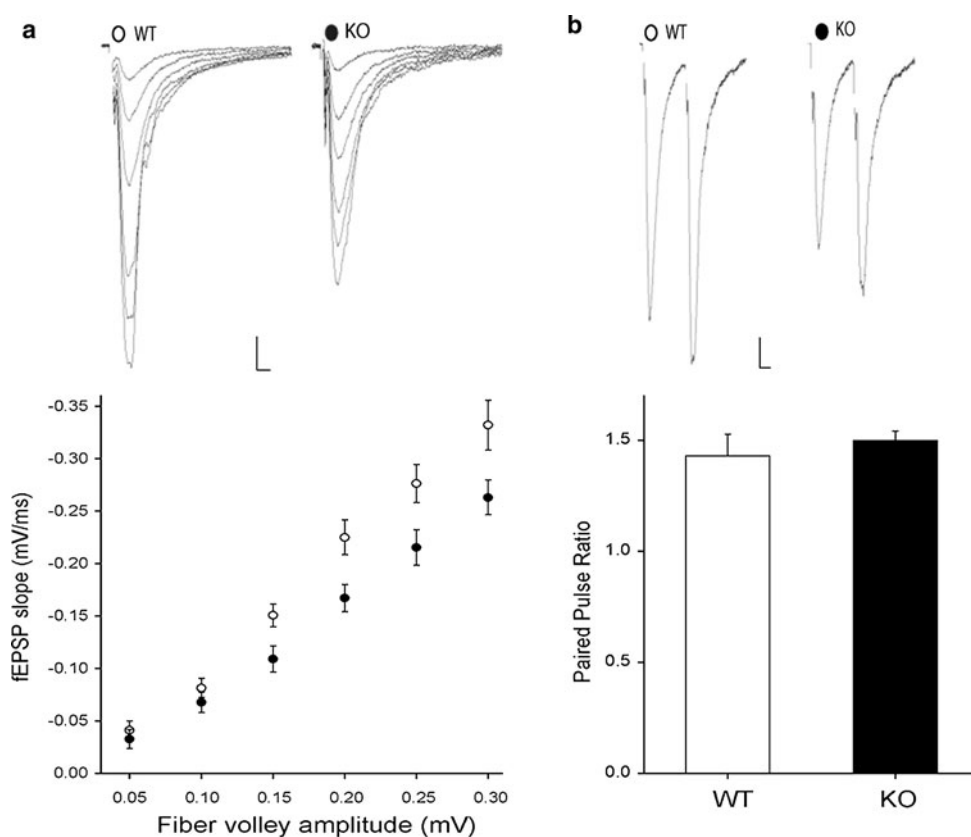
We then investigated whether changes in Gria2 expression, editing and splicing affect basal AMPAR-mediated synaptic transmission in hippocampal slices from 4-week-old Rsk2KO mice. To assess the strength of synaptic transmission, we compared the size of the presynaptic fiber volley (input) to the slope of the EPSP (output) in striatum radiatum and found a 25% significant reduction in Rsk2KO ( $n = 9$ ) mice when compared with WT littermates ( $n = 7$ ) (Fig. 6a). We evaluated also paired-pulse facilitation (PPF), a measure of release probability from presynaptic terminals. The PPF curves were essentially identical in slices from control and Rsk2KO mice (Fig. 6b) indicating that RSK2 most likely modulates AMPA neurotransmission postsynaptically with no effect on presynaptic function.

## Discussion

The absence of gross structural alterations in the brain of Rsk2KO mice strongly indicates that their defective cognitive phenotype should be linked to subtler molecular or cellular alterations. In an effort to identify such alterations, we carried out a detailed characterization of the differences existing between the transcriptional profiles of the hippocampus of WT and KO animals. Our analysis by oligonucleotide microarrays yielded a list of 100 differentially expressed genes with high degree of statistical significance. These results were further confirmed for 24 genes by quantitative RT-PCR demonstrating their robustness.

Our study revealed a great variety of RSK2-influenced genes acting in various biological pathways. Indeed, the network with the highest score (as determined by ingenuity pathway analysis) centers on the NF complex, which plays a prominent role in cell differentiation and proliferation and apoptosis (Brand et al. 1997). Twelve genes are implicated at various stages of the cell cycle in Rsk2KO neurons (including *Ubp1*, *Rb1*, *Max*, *Sod2*, and *Ptgs2*). This result suggests strongly that abnormal cell proliferation contributes to the CLS phenotype. In addition, 34 of the altered genes have been implicated in cell death or survival, out of which 7 (*Acng8*, *Diablo*, *Gria2*, *Ubp1*, *Ptgs2*, *Rb1*, *Sod2*) have been specifically associated with neuronal cell death. Interestingly, previous studies suggested that apoptotic and antiapoptotic cascades are tightly associated with cognitive dysfunctions and neurological disorders (Lutz 2007). Further studies are, therefore, necessary to investigate cell proliferation and death in Rsk2KO mice. Four genes, including *Sod2*, *Fxn*, *Gmfb* and *Cp* are implicated in free radical scavenging, suggesting also a possible involvement of free radicals in the

**Fig. 6 Patch-clamp analysis**  
 Input-output curves for basal synaptic transmission in hippocampal slices. As illustrated in the sample traces and the graph, for each input (fiber volley  $\geq 0.15$  mV), the output (fEPSP) is reduced by 25% in Rsk2KO slices ( $p \leq 0.05$ , WT  $n = 10$ ; KO  $n = 9$ ). Scale bar 0.1 mV, 5 ms. **b** Paired-pulse facilitation (PPF) does not differ between Rsk2KO ( $n = 9$ ) and WT ( $n = 6$ ) cells. Sample traces are illustrated above the bar graph. Scale bar 0.05 mV, 10 ms



CLS phenotype. Ten genes (among which *Gria2*, *Igf1*, *Ptgs2*, *Sod2*, *Nptxr*, *Ahr* and *Vtn*) play a role in nervous system development and function. IGF1 for instance is essential for normal dendritic growth (Cheng et al. 2003). NPTXR is thought to be involved in activity-dependent synaptic plasticity (Xu et al. 2003). The AHR homologs in *Drosophila*, *Spineless* (*Ss*), and in *Caenorhabditis elegans* *ahr-1*, regulate dendrite morphology (Kim et al. 2006) and neuronal differentiation (Qin and Powell-Coffman 2004). The expression of a number of genes involved in neurotransmission was also found affected. Up-regulation of *Vamp4* and *Stxbp3* genes in mutant mice points to a role of RSK2 in pre-synaptic vesicle trafficking (Wang and Tang 2006). Up-regulation of *Cacnb4* encoding a  $\beta$ -subunit of Voltage-gated  $Ca^{++}$  channels, suggests that direct influence of RSK2 on  $Ca^{++}$  influx into the cell upon membrane polarization is regulated via RSK2 (Birnbaumer et al. 1998). Moreover, alteration of *Gnb1* and *Gria2* expression suggests that RSK2 is involved in glutamate receptor signaling. GNB1 mediates the fast voltage-dependent inhibition of N-type  $Ca^{++}$  channels (Fu and Cheung 1999). The function of *Gria2* will be discussed below. Finally, the expression of several genes encoding proteins implicated in gene expression was altered in Rsk2KO hippocampi (including *Etv3*, *Hip2*, *Rb1*, *Irf2*, *Max*, *Runx2* and *Trip11*) suggesting that some of the RSK2

effects may be direct and others indirect. Strikingly, two of the genes with altered expression in Rsk2KO hippocampi, *Lamp2* and *Cul4b*, have previously been associated with syndromic forms of X-linked mental retardation (Nishino et al. 2000; Zou et al. 2007).

Among the genes associated with a specific neuronal function, *Gria2* was of particular interest because GLUR2 controls the key biophysical properties of AMPA receptors, which are implicated in learning and memory (Kessels and Malinow 2009). Most excitatory synaptic transmission in the brain being mediated through AMPAR, changes in the properties of these receptors are likely to have a major impact on brain function. Furthermore, GLUR2 was shown to bind directly to RSK2 in murine neurons suggesting a direct influence of RSK2 on GLUR2 function (Thomas et al. 2005). The GLUR family contains four closely related members (GLUR1-4). AMPARs are tetrameric, composed of various combinations of GLUR1-4 subunits, and the conductance properties of the receptors are highly dependent on their subunit composition (Kuner et al. 2001). GLUR2-lacking receptors have a higher  $Ca^{++}$  permeability, channel conductance, open probability and inactivation time course compared to GLUR2-containing receptors (Isaac et al. 2007). Therefore, the presence or absence of the GLUR2 subunit can dramatically alter AMPAR properties and thereby synaptic transmission.

Our results provide evidence that in the hippocampus of LTP and LTD. The signaling mechanisms involved in the Rsk2KO mice total expression of GLUR2 is increased, and increased levels of transcription of *Gria2* in Rsk2KO mice that the expression is also increased at the surface of synaptically hippocampal neurons are not yet known. The regulation of AMPARs in cultured primary hippocampal cells. It was reported previously that surface insertion of GLUR2 occurs constitutively under basal conditions (Passafium et al. 2001). Our results are compatible with these data. It may be that the proximal region of the promoter (Borges and Dingledine 2001). RNA editing is mediated by adenosine deaminase acting on RNA (ADAR) enzymes. Three structurally related ADARs (ADAR1 to ADAR3) have been identified in mammals. ADAR2 predominantly catalyzes RNA editing at the Q/R site of GLUR2 (Peng et al. 2006), whereas it

The Q/R site was completely edited in both WT and Rsk2KO hippocampi, whereas the extent of R/G editing mechanism of the R/G editing dysregulation may be caused by altered function or expression of one or several ADAR enzymes. However, the fact that editing of the Q/R site in Rsk2KO mice is not affected in Rsk2KO mice suggesting that ADAR2 is excluded. Further investigations are necessary to determine precisely the molecular events leading to up-regulation of the Q/R site in postnatal brain. Our results in WT mice show that Q/R editing is not altered in Rsk2KO mice. GLUR2-4 undergo also RNA editing [arginine (R) to glycine (G)] at amino acid position 743 (Lomeli et al. 1994). The presence of edited GLUR2 subunits at position 743 yields channels with faster kinetics. This gene encodes a synaptic protein, TARPP-8 that participates in consolidation phase assembly and surface expression of AMPAR complexes of memory and is involved in modulating neurotransmitter release. Evidence was provided that TARPP-8 is critical for Rsk2KO mice. Finally, alternative splicing in the extracellular domain of the AMPARs generates two isoforms in the hippocampus (Rouach et al. 2005). Up-regulation of  $\beta$ ip and  $\beta$ op. Native AMPAR are heteromeric assemblies of different subunits that may have different functions.

The data in this study provide a first glimpse of the gene expression profile of adult hippocampi in the absence of RSK2 expression. However, the Rsk2KO animals represent a valuable model to study human CofPNDLowry syndrome, it has significant limitations due to potential alteration of R/G editing and splicing of GLUR2 in Rsk2KO mice are therefore expected to alter AMPARs channel kinetics, desensitization and trafficking. Further functional studies based on this technology could offer further clues about the function of RSK2.

In conclusion, functional impairment of neurotransmission and plasticity due to AMPAR dysfunction may, indeed, contribute to the cognitive deficits in Rsk2KO mice. However, further investigations are necessary to determine precisely the molecular events leading to alteration of GLUR2 expression and the contribution of this dysregulation to the cognitive dysfunction. The involvement of other pathways, including in particular cellular proliferation and apoptosis, remains also to be investigated.

Finally, the genes identified by our microarray analysis will help in further unravel the various functions of RSK2 in the hippocampus can be speculated to play a role in the pathogenesis of mental retardation in Coffin-Lowry syndrome and may provide targets for pharmaceutical intervention.

#### Accession number

The data of the expression arrays produced for this report have been submitted to NCBI's Gene Expression Omnibus (GEO: <http://www.ncbi.nlm.nih.gov/geo/>) and are accessible through GEO Series accession number GSE22137.

**Acknowledgments** The authors wish to thank Jessica Heringer for technical assistance and helpful discussions, and the IGBMC, Institut de Génétique et de Biologie Moléculaire et Cellulaire for assistance. This work was supported by the French National Agency for Research (Grant number 08-MNPS-021-01, to A.H.), the Fondation de Lejeune (to A.H.), the Centre National de la Recherche Scientifique, the Institut National de la Santé et de la Recherche, the Collège de France and the University of Strasbourg. AS was supported by a fellowship from the Ministère pour la Recherche et Technologie of France and TM by a scholarship from the Higher Education Commission (HEC) of Pakistan.

**Conflict of interest** The authors declare that they have no conflict of interest.

#### References

- Benjamini Y, Hochberg Y (1995) Controlling the false discovery rate: a practical and powerful approach to multiple testing. *J R Stat Soc B* 57:289–300
- Birnbaumer L, Qin N, Olcese R, Tareilus E, Platano D, Costantin J, Stefani E (1998) Structures and functions of calcium channel beta subunits. *J Bioenerg Biomembr* 30:357–375
- Borges K, Dingledine R (2001) Functional organization of the GluR1 glutamate receptor promoter. *J Biol Chem* 276:25929–25938
- Brand K, Page S, Walli AK, Neumeier D, Baeuerle PA (1997) Role of nuclear factor-kappa B in atherogenesis. *Exp Physiol* 82:297–304
- Brorson JR, Li D, Suzuki T (2004) Selective expression of heteromeric AMPA receptors driven by  $\beta$ ip- $\beta$ op differences. *J Neurosci* 24:3461–3470
- Carlson NG, Howard J, Gahring LC, Rogers SW (2000) RNA editing (Q/R site) and  $\beta$ op/ $\beta$ ip splicing of AMPA receptor transcripts in young and old brains. *Neurobiol Aging* 21:599–606
- Cheng CM, Mervis RF, Niu SL, Salem N Jr, Witters LA, Tseng V, Reinhardt R, Bondy CA (2003) Insulin-like growth factor 1 is essential for normal dendritic growth. *J Neurosci Res* 73:1–9
- Davis S, Laroche S (2006) Mitogen-activated protein kinase/extracellular regulated kinase signalling and memory stabilization: a review. *Genes Brain Behav* 5(Suppl 2):61–72
- De Cesare D, Jacquot S, Hanauer A, Sassone-Corsi P (1998) Rsk2 activity is necessary for epidermal growth factor-induced phosphorylation of CREB protein and transcription of c-fos gene. *Proc Natl Acad Sci USA* 95:12202–12207
- Fredin M, Gammeltoft S (1999) Role and regulation of 90 kDa ribosomal S6 kinase (RSK) in signal transduction. *Mol Cell Endocrinol* 151:65–77
- Fu AK, Cheung WM (1999) Identification of genes induced by neuregulin in cultured myotubes. *Mol Cell Neurosci* 14:241–253
- Ghate A, Befort K, Becker JA, Filliol D, Bole-Feysot C, Demebele D, Jost B, Koch M, Kieffer BL (2007) Identification of novel striatal genes by expression profiling in adult mouse brain. *Neuroscience* 146:1182–1192
- Guimiot F, Delezoide AL, Hanauer A, Simonneau M (2004) Expression of the RSK2 gene during early human development. *Gene Expr Patterns* 4:111–114
- Hanauer A, Young ID (2002) Coffin-Lowry syndrome: clinical and molecular features. *J Med Genet* 39:705–713
- Isaac JT, Ashby M, McBain CJ (2007) The role of the GluR2 subunit in AMPA receptor function and synaptic plasticity. *Neuron* 54:859–871
- Kessels HW, Malinow R (2009) Synaptic AMPA receptor plasticity and behavior. *Neuron* 61:340–350
- Kim MD, Jan LY, Jan YN (2006) The bHLH-PAS protein Spineless is necessary for the diversification of dendrite morphology of Drosophila dendritic arborization neurons. *Genes Dev* 20:2773–2778
- Kuner T, Beck C, Sakmann B, Seeburg PH (2001) Channel-lining residues of the AMPA receptor M2 segment: structural environment of the Q/R site and identification of the selectivity filter. *J Neurosci* 21:4162–4172
- Lai F, Chen CX, Carter KC, Nishikura K (1997) Editing of glutamate receptor B subunit ion channel RNAs by four alternatively spliced DRADA2 double-stranded RNA adenosine deaminases. *Mol Cell Biol* 17:2413–2424
- Lee JC, Greig A, Ravindranathan A, Parks TN, Rao MS (1998) Molecular analysis of AMPA-specific receptors: subunit composition, editing, and calcium influx determination in small amounts of tissue. *Brain Res Protoc* 3:142–154
- Lomeli H, Mosbacher J, Melcher T, Geiger JR, Kuner T, Monyer H, Higuchi M, Bach A, Seeburg PH (1994) Control of kinetic properties of AMPA receptor channels by nuclear RNA editing. *Science* 266:1709–1713
- Lutz RE (2007) Trinucleotide repeat disorders. *Semin Pediatr Neurol* 14:26–33
- Malinow R, Malenka RC (2002) AMPA receptor trafficking and synaptic plasticity. *Annu Rev Neurosci* 25:103–126
- Marques Pereira P, Gruss M, Braun K, Foos N, Pannetier S, Hanauer A (2008) Dopaminergic system dysregulation in the *mrsk2\_KO* mouse, an animal model of the Coffin-Lowry syndrome. *J Neurochem* 107:1325–1334
- Nakamoto N, Nalavadi V, Epstein MP, Narayanan U, Bassell GJ, Warren ST (2007) Fragile X mental retardation protein deficiency leads to excessive mGluR5-dependent internalization of AMPA receptors. *Proc Natl Acad Sci USA* 39:15537–15542
- Nishino I, Fu J, Tanji K, Yamada T, Shimojo S, Koori T, Mora M, Riggs JE, Oh SJ, Koga Y et al (2000) Primary LAMP-2 deficiency causes X-linked vacuolar cardiomyopathy and myopathy (Danon disease). *Nature* 406:906–910
- Passafaro M, Pith V, Sheng M (2001) Subunit-specific temporal and spatial patterns of AMPA receptor exocytosis in hippocampal neurons. *Nat Neurosci* 4:917–926
- Pei W, Huang Z, Wang C, Han Y, Park JS, Niu L (2009) Flip and  $\beta$ op: a molecular determinant for AMPA receptor channel opening. *Biochemistry* 48:3767–3777
- Peng PL, Zhong X, Tu W, Soundarapandian MM, Molner P, Zhu D, Lau L, Liu S, Liu F, Lu Y (2006) ADAR2-dependent RNA editing of AMPA receptor subunit GluR2 determines vulnerability of neurons in forebrain ischemia. *Neuron* 49:719–733

- Poirier R, Jacquot S, Vaillend C, Souththiphong AA, Libbey M, Davis Thomas GM, Rumbaugh GR, Harrar DB, Haganir RL (2005) S, Laroche S, Hanauer A, Welzl H, Lipp HP, Wolfer DP (2007) Deletion of the Coffin-Lowry syndrome gene Rsk2 in mice is associated with impaired spatial learning and reduced control of exploratory behavior. *Behav Genet* 37:31–50
- Qin H, Powell-Coffman JA (2004) The *Caenorhabditis elegans* hydrocarbon receptor, AHR-1, regulates neuronal development. *Dev Biol* 270:64–75
- Rouach N, Byrd K, Petralia RS, Elias GM, Adesnik H, Tomita S, Karimzadegan S, Kealey C, Brecht DS, Nicoll RA (2005) TARP gamma-8 controls hippocampal AMPA receptor number, distribution and synaptic plasticity. *Nat Neurosci* 8:1525–1533
- Sassone-Corsi P, Mizzen CA, Cheung P, Crosio C, Monaco L, Jacquot S, Hanauer A, Allis CD (1999) Requirement of Rsk-2 for epidermal growth factor-activated phosphorylation of histone H3. *Science* 285:886–891
- Seidenman KJ, Steinberg JP, Haganir R, Malinow R (2003) Glutamate receptor subunit 2 serine 880 phosphorylation modulates synaptic transmission and mediates plasticity in CA1 pyramidal cells. *J Neurosci* 23:9220–9228
- Wang Y, Tang BL (2006) SNAREs in neurons beyond synaptic vesicle exocytosis. *Mol Membr Biol* 23:377–384
- Xu D, Hopf C, Reddy R, Cho RW, Guo L, Lanahan A, Petralia RS, Wenthold RJ, O'Brien RJ, Worley P (2003) Narx and NP1 form heterocomplexes that function in developmental and activity-dependent synaptic plasticity. *Neuron* 39:513–528
- Zeniou M, Ding T, Trivier E, Hanauer A (2002) Expression analysis of RSK gene family members: the RSK2 gene, mutated in Coffin-Lowry syndrome, is prominently expressed in brain structures essential for cognitive function and learning. *Hum Mol Genet* 11:2929–2940
- Zou Y, Liu Q, Chen B, Zhang X, Guo C, Zhou H, Li J, Gao G, Guo Y, Yan C et al (2007) Mutation in CUL4B, which encodes a member of cullin-RING ubiquitin ligase complex, causes X-linked mental retardation. *Am J Hum Genet* 80:561–566